Calibration of resistance factors for design of deep foundations against lateral deflections

He, Pengpeng; Fenton, Gordon A.; Griffiths, D. V.

Published in:
Computers and Geotechnics

DOI:
10.1016/j.compgeo.2023.105250

Publication date:
2023

Calibration of resistance factors for design of deep foundations against lateral deflections

Pengpeng He [a]

[a] Department of Engineering Mathematics, Dalhousie University, Halifax, NS, Canada.

Email: pengpeng.he@dal.ca

Gordon A. Fenton [b] (corresponding author)

[b] Department of Engineering Mathematics, Dalhousie University, Halifax, NS, Canada.

Email: gordon.fenton@dal.ca

D. V. Griffiths [c]

[c] Department of Civil and Environmental Engineering, Colorado School of Mines, Golden, CO, USA.

Email: d.v.griffiths@mines.edu

Funding: This work was supported by the Canadian Standard Association Group Research Project Award and Mitacs [grant numbers IT21047]; and the Natural Sciences and Engineering Research Council of Canada.

Word count: 6733 (texts) + (10+2)*250 = 9733 (10 figures and 2 tables, including captions but excluding this title page)

Abstract: In geotechnical engineering, the load and resistance factor design (LRFD) approach has been recommended as an alternative to the global factor of safety method. In this paper, the geotechnical resistance factors for the ultimate and serviceability limit states (ULS and SLS) of laterally loaded piles under wind loading are calibrated using a reliability-based method. Both cohesive and frictional soils are considered. Parametric studies are performed to investigate the effects of various parameters on the estimated failure probability, and the required resistance factors for ULS and SLS are provided. The results indicate that the effect of the limiting maximum pile head deflection on the required resistance factor is negligible and that the "worst case" correlation length depends on the pile length. In addition, the required resistance factor for ULS design is 0.55 to 0.78, suggesting that the value of ϕ_g=0.50 stipulated by geotechnical code provisions in Canada is relatively conservative. Considering the target lifetime failure probability of 0.01 for SLS, the required resistance factor is around 0.60 for both clay and sand, which is smaller than the recommendation of ϕ_g=0.80 by the design codes in Canada.

Key words: Load and resistance factor design; reliability analysis; lateral deflection; resistance factor; laterally loaded piles

1 Introduction

In addition to the vertical geotechnical resistance and the structural safety of piles associated with pile material properties, the design of deep foundations subjected to lateral loading should also satisfy ultimate limit state (ULS) and serviceability limit state (SLS) requirements (Duncan et al., 1994). Traditionally, deterministic methods based on a global factor of safety are employed for the design of piles against lateral deflections. The load and resistance factor design (LRFD) approach is a more recent alternative, where separate factors are given to the geotechnical resistance and the load effects. Examples of modern LRFD in geotechnical design codes can be found in the Canadian Highway Bridge Design Code (CHBDC) (CSA, 2019), the AASHTO (2020), and the Canadian Foundation Engineering Manual (CFEM) (Canadian Geotechnical Society, 2006), although the last is not a design code.

The resistance factor in the LRFD is applied to account for the variability in the geotechnical resistance, and is generally calibrated using reliability analyses (e.g., Ellingwood et al., 1982; Barker et al.,1991; Phoon et al., 2000; Fenton et al., 2008). The calibration of resistance factors for the bearing capacity and vertical settlement

of deep foundations can be found in the literature (e.g., Naghibi et al., 2004; Haldar and Sivakumar Babu, 2008; Foye et al., 2009; Kwak et al., 2010; Naghibi and Fenton, 2011; Tang and Phoon, 2018). Although the CHBDC (CSA, 2019) specifies the ULS and SLS resistance factors for laterally loaded piles, there is still a lack of calibration of these resistance factors. Kim et al. (2021) and Kim and Lee (2022) calibrated the resistance factors for laterally loaded piles in sands based on a number of lateral load test results, although the variability in soil properties was not directly considered. Low (2020) performed reliability analyses for laterally loaded piles using the first-order reliability method (FORM), where the soil properties are assumed to be single random variables taken from specific distributions without considering the spatial variability of the soil. Griffiths et al. (2013) carried out a reliability analysis of a beam on a spatially random elastic foundation but not in the LRFD framework. The aim of this paper is to calibrate the ULS and SLS resistance factors needed for laterally loaded piles using the Random Finite Element Method (RFEM).

Generally, the SLS of a laterally loaded pile refers to pile deflections exceeding the maximum tolerable deflection, and the ULS can refer to the ultimate capacity of the soil around the pile or excessive pile deflections resulting in ULS failure of the structure it supports. In most cases, the soil ultimate capacity is unlikely to be reached (Duncan et al., 1994), and thus the pile deflection criterion is considered for both ULS and SLS of a laterally loaded pile within the LRFD framework. The general LRFD equation is expressed as

$$\phi_g \hat{R} \geq \sum_{i=1}^{n} \alpha_i \hat{F}_i \tag{1}$$

where ϕ_g is the geotechnical resistance factor for ULS or SLS; $\hat{R}$ is the characteristic lateral soil resistance; $\hat{F}_i$ is the i^{th} characteristic lateral load; and α_i is the corresponding load factor. The National Building Code of Canada (NBCC) (National Research Council, 2015) provides a series of load combinations for design in terms of dead, live, snow, wind, and earthquake loads. In this paper, only wind loads are considered for the design of pile lateral deflections.

In the paper, the LRFD framework (i.e., random soil and load models, random finite element model, and foundation design) for a laterally load pile is first introduced, and the failure probability is then estimated for ULS and SLS. An example pile under wind loading is designed, and parametric studies are carried out to investigate the effects of various parameters. The required resistance factors for ULS and SLS are also

provided and compared to those specified by current geotechnical design codes. Conclusions and recommendations for further research are provided at the end of the paper.

2 Random finite element method

2.1 Random soil and load models

This paper separately considers undrained and drained soil conditions. For undrained soil conditions, the soil strength is characterized by the undrained shear strength, s_u, which is represented by a random field. Since s_u is non-negative, its random field is assumed to follow a lognormal distribution, having a mean μ_{s_u} and a standard deviation σ_{s_u}. To transfer a lognormally distributed field to its normally distributed counterpart, $\ln s_u$, the following relationships are used

$$\sigma^2_{\ln s_u} = \ln\left(1+\nu^2_{s_u}\right)$$
$$\mu_{\ln s_u} = \ln\left(\mu_{s_u}\right) - \frac{1}{2}\sigma^2_{\ln s_u} \quad (2)$$

where $\nu_{s_u} = \sigma_{s_u} / \mu_{s_u}$ is the coefficient of variation of s_u.

For drained soil conditions, the soil strength is characterized by the internal friction angle, ϕ', which here is assumed to be bounded between 25° and 45°, following a marginal tanh distribution with a scale parameter governing the variability of ϕ' between the two bounds (Fenton and Griffiths, 2008). The coefficient of variation of ϕ' for sands ranges from 0.05 to 0.15 (Lee et al., 1983; Phoon and Kulhawy, 1999). In this study, three values of $\nu_{\phi'}$ are considered, i.e., $\nu_{\phi'} = 0.05$, 0.10, and 0.15, corresponding to scale parameters of 1.22, 2.58, and 4.35, respectively.

The correlation coefficient, ρ, between s_u (or ϕ') at one spatial location, $\underset{\sim}{x}_i$, and at a second location, $\underset{\sim}{x}_j$, is described by a correlation function. An isotropic Markovian correlation function (e.g., Vanmarcke, 2010), having the following form, is considered in this study

$$\rho\left(\tau_{ij}\right) = \exp\left(\frac{-2\tau_{ij}}{\theta}\right) \quad (3)$$

where $\tau_{ij} = \left|\underset{\sim}{x}_i - \underset{\sim}{x}_j\right|$ is the absolute distance between the two points in the soil mass; and θ is the spatial correlation length. Note that the correlation length for the s_u random field acts between values of $\ln s_u$. However, it has been shown that the log-space correlation length and its real-space counterpart result in very

similar results for most cases in practice and the distinction is not particularly important given the significant uncertainty in correlation lengths (e.g., Burgess et al., 2019; Puła and Griffiths, 2021). Similarly, for drained soil conditions, the correlation length is assumed to act between points in the underlying Gaussian field, which is then transformed into the friction angle field. See Fenton and Griffiths (2008) for details. As in the case for the undrained case, the correlation lengths in the friction angle field and its underlying Gaussian field will be very similar.

It should be noted that although soils generally exhibit an anisotropic correlation structure, where the vertical correlation length is generally smaller than the horizontal correlation length, the development of code provisions must conservatively take into consideration cases where this is not the case at a particular site. In addition, for lateral loading, the stiffness of the pile itself will result in averaging out much of the vertical variability in the soil properties. In other words, assuming a small correlation length in the vertical direction will be unconservative. This paper assumes an isotropic correlation structure. The worst case correlation length will always be about the pile length in any case.

In this paper, for simplicity, the horizontal load acting on the pile head is assumed to be only wind loading, F_W, which is assumed to be lognormally distributed, having a mean of μ_W and a standard deviation of σ_W.

2.2 Random finite element model for laterally loaded piles

2.2.1 p-y method

The *p-y* method (e.g., McClelland and Focht, 1958) has been widely accepted to predict pile lateral deflections under lateral static and cyclic loads, since the nonlinear *p-y* curve is able to account for a wide range of soil and loading conditions. The *p-y* curve specifies the relationship between the pile deflection, *y*, and the corresponding soil lateral pressure, *p*, at any pile depth, as shown in Figure 1.

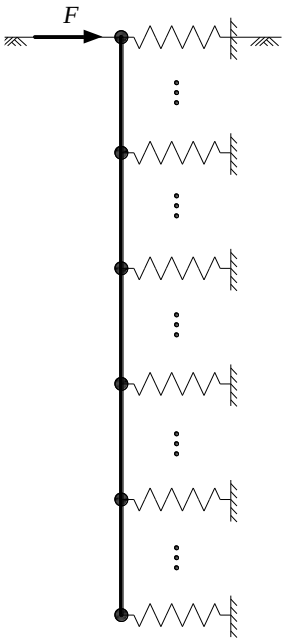

Figure 1. Schematic of the *p-y* method

The nonlinear *p-y* relationship depends highly upon the soil type, soil shear strength, overburden pressure, pile diameter and loading conditions. In this paper, only static lateral loads are considered, and cohesive and frictional soils are separately investigated. API (2014) specifies that the lateral capacity and *p-y* curve for stiff clays (s_u>100 kPa) are similar to those for soft clays under static loading conditions. Therefore, the *p-y* curve recommended by API (2014) for soft clays is adopted for cohesive soils regardless of the consistency of clay. The *p-y* curve suggested by API (2014) for clays is based on the equation of Matlock (1970), although the API model makes use of piece-wise curves for Matlock's (1970) equation, as detailed in Figure 2.

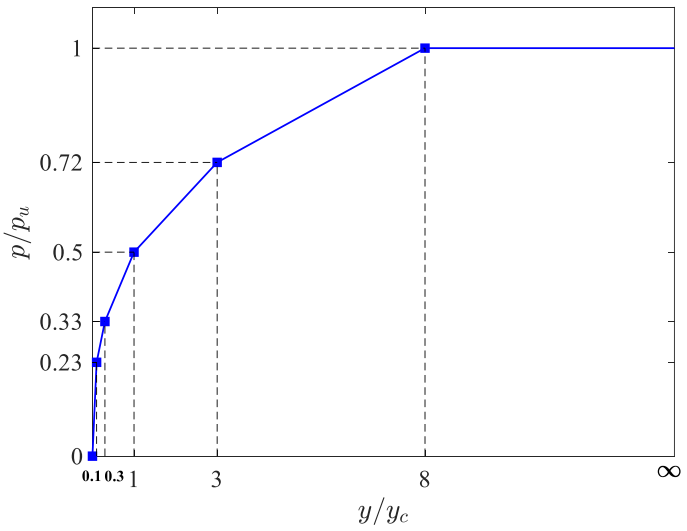

Figure 2. Piece-wise *p-y* curves recommended by API (2014) for cohesive soils

The ultimate lateral pressure, p_u, shown in Figure 2 is evaluated as the minimum of

(4a) $$p_u = 3s_u D + \gamma z D + J s_u z$$

or

(4a) $$p_u = 9 s_u D$$

where D is the pile diameter; γ is the soil unit weight; z is the depth below the ground level; and J is an empirical coefficient depending on the soil shear strength, which is taken to be 0.5 in this study. In Figure 2, y_c is the corrected deflection at one-half the ultimate lateral pressure, and is calculated using

(5) $$y_c = 2.5 \varepsilon_{50} D$$

where ε_{50} is the strain at one-half the maximum deviator stress for an undrained triaxial compression test, depending on the soil undrained shear strength. ε_{50} is taken to be 0.01 in this analysis.

For sands, the *p*-*y* relationship recommended by API (2014) is expressed as

(6) $$p = A p_u \tanh\left[\frac{kz}{A p_u} y\right]$$

where A is a factor accounting for loading conditions, defined as $A = (3.0 - 0.8 z/D) \geq 0.9$ for static loading; k is the rate of increase with depth of the initial modulus of subgrade reaction, depending on the soil internal friction angle. API (2014) provides the k values for four specific soil internal friction angles (see the square symbols in Figure 3), which are well fitted by the following exponential function, also shown in Figure 3.

(7) $$k = 0.1549 \exp(0.1418 \phi') \qquad (\phi' \text{ in degrees})$$

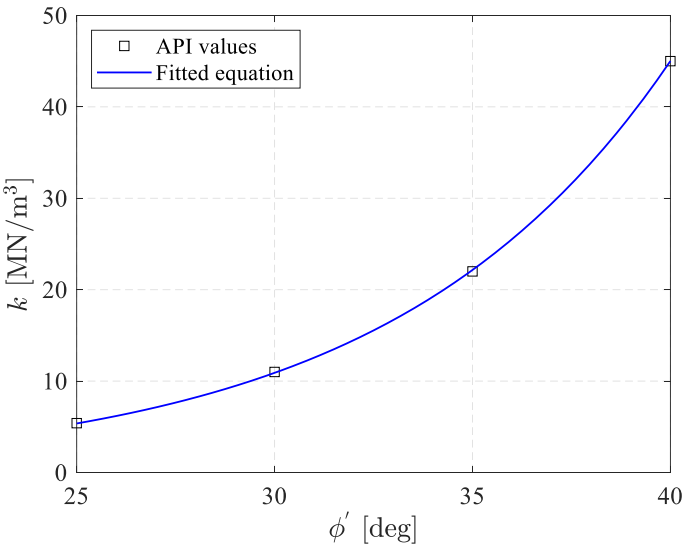

Figure 3. Fitted equation for parameter k used in the *p*-*y* curve for sand

The ultimate lateral pressure for sand is computed to be the minimum of

(8a) $$p_u = (C_1 z + C_2 D) \gamma z$$

or

(8a) $$p_u = C_3 D \gamma z$$

where C_1, C_2 and C_3 are coefficients determined as functions of the sand internal friction angle, ϕ', i.e.,

(9)
$$C_1 = \frac{(\tan\beta)^2 \tan\alpha}{\tan(\beta-\phi')} + K_0\left[\frac{\tan\phi'\sin\beta}{\cos\alpha\tan(\beta-\phi')} + \tan\beta(\tan\phi'\sin\beta - \tan\alpha)\right]$$
$$C_2 = \frac{\tan\beta}{\tan(\beta-\phi')} - K_a$$
$$C_3 = K_a\left[(\tan\beta)^8 - 1\right] + K_0\tan\phi'(\tan\beta)^4$$

and where $\alpha = \phi'/2$; $\beta = 45^\circ + \phi'/2$; $K_0 = 0.4$; and $K_a = (1-\sin\phi')/(1+\sin\phi')$.

2.2.2 Random finite element model

In this paper, the Random Finite Element Method (RFEM) (Fenton and Griffiths, 1993; Griffiths and Fenton, 1993) was used to estimate the lateral deflection reliability of a free-head pile subject to lateral loading at the ground line. The programme, 'rpyspile', used in this study is based on the one-dimensional *p-y* finite element model developed by Smith and Griffiths (1988). The programme employs one-dimensional 2-node beam elements to model the pile and horizontal *p-y* springs to model the soil stiffness using local average subdivision (LAS) (Fenton and Vanmarcke, 1990), as illustrated in Figure 4. The approach is similar to that described by Fenton and Griffiths (2007) using rod elements for the vertically loaded pile and *t-z* springs for the soil. The pile mesh is consistent with the soil mesh in the vertical direction, and the *p-y* curve for each pile node is generated based on the local soil properties (at the pile location) using the *p-y* method described previously. It should be noted that the lateral pile behavior (*p-y* curves) is governed by a certain range of soil on the back and front sides of the pile. For simplicity, the soil properties at the pile location are taken as the average soil properties in the soil cells on either side of the pile in order to generate the *p-y* curves. A 2-D soil mass is generated in order to allow for virtual sampling of the soil and estimate soil properties for the design. The virtual sampling is performed simply by sampling the random field along a column of depth *d* located a distance *s* from the pile, as shown in Figure 4.

In this study, the pile is assumed to have a constant circular cross-section along the pile length. The unit weight of the soil, γ, the pile length, L, and the pile elastic modulus, E_p, are assumed to be deterministic, and only the

soil strength parameters (i.e., s_u for clay and ϕ' for sand) are assumed to be random and spatially variable, as discussed previously.

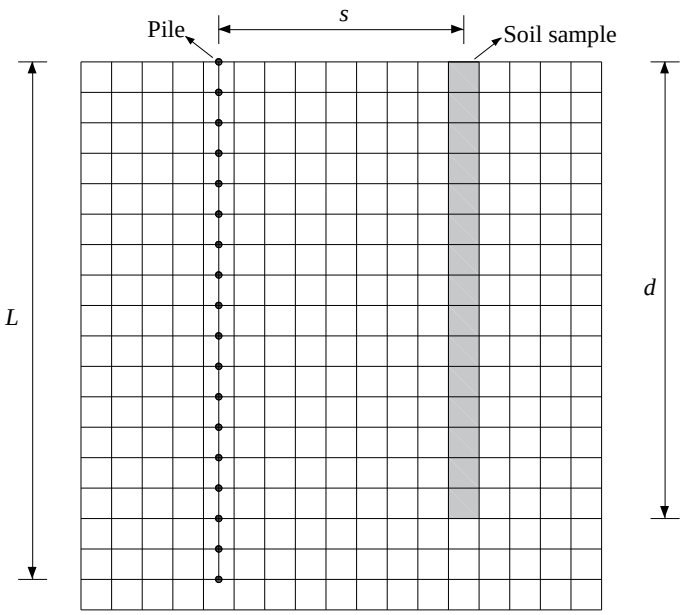

Figure 4. Schematic pile and soil sampling

3 Foundation design

Preliminary analyses conducted by the authors have shown that vertical axial loads on the pile have a negligible effect on the calculated pile head deflection, therefore, in the following analysis, the vertical load on the pile is not considered. The design lateral load, $\alpha_W \hat{F}_W$, acting on the pile head is assumed to be wind loading. The characteristic wind load, $\hat{F}_W$, is estimated here to be $\hat{F}_W = \mu_W / k_W$, where k_W is the bias factor for wind loads. The bias factor is taken to be k_W=0.78, following the recommendation of Ellingwood (1981).

In this study, the pile length, L, is held constant, while the pile diameter, D, is designed to satisfy the LRFD inequality. The *p-y* programme can only calculate the lateral soil reaction for a given pile diameter but is not able to perform the inverse procedure required to determine the pile diameter for a given lateral load. To facilitate pile design, a series of deterministic cases involving a range of soil strength parameters and pile diameters were performed, and the relationships between the lateral soil reaction, soil strength parameters and pile diameters for a specific pile length and pile elastic modulus were established using curve fitting.

A wide range of pile diameters, D (0.4 ~ 2.0 m), undrained shear strengths, s_u (20 ~ 180 kPa), and internal friction angles, ϕ' (25° ~ 45°), were taken in this analysis. In addition, three limiting pile deflections at pile head are prescribed, that is, y_m=25 mm, 50 mm, and 75 mm. The pile length and elastic modulus are held constant at L=10 m and E_p=35 GPa, respectively. The soil unit weight is 20 kN/m^3. For each deterministic

case, the lateral resistance at pile head, R, is evaluated using the above-mentioned p-y programme. The form of the equation used to fit the relationship between R, s_u (or ϕ'), and D is expressed as

$$R = a\left[1-\exp\left(bD^c\right)\right] \tag{10}$$

where a, b and c are the fitted coefficients determined as functions of s_u for clay and ϕ' for sand, as follows

$$\begin{aligned} a(s_u) &= p_1(s_u)^2 + p_2 s_u + p_3 \\ b(s_u) &= p_4 \qquad \text{for clay} \\ c(s_u) &= \frac{q_1 s_u + q_2}{s_u + q_3} \end{aligned} \tag{11a}$$

$$\begin{aligned} a(\phi') &= \exp\left[p_1(\phi')^2 + p_2\phi' + p_3\right] \\ b(\phi') &= \frac{q_1(\phi')^2 + q_2\phi' + q_3}{\phi' + q_4} \qquad \text{for sand } (\phi' \text{ in radians}) \\ c(\phi') &= p_4 \end{aligned} \tag{11b}$$

The fitting coefficients, p_1, p_2, p_3, p_4, q_1, q_2, q_3, q_4, shown in Eq. (11) for different limiting pile head deflections are summarized in Table 1, and the comparison between the calculated finite element results and the fitted equation (i.e., Eq. (10)) are shown in Figure 5. It can be seen that the fitted equation shows very satisfactory agreement with the finite element results for both clay and sand.

Table 1. Fitting coefficients for various limiting pile head deflections

Soil	y_m **[mm]**	p_1	p_2	p_3	p_4	q_1	q_2	q_3	q_4
Clay	25	-0.008820	11.12	134.69	-0.863	2.871	258.27	218.05	
	50	-0.01010	14.33	156.65	-0.946	3.349	512.31	429.83	
	75	-0.01093	16.61	175.13	-0.969	3.925	870.22	746.38	
Sand	25	0.8158	6.954	3.366	2.263	-1.879	3.939	-2.137	0.2443
	50	0.6409	6.573	4.196	2.292	-0.1300	0.8040	-0.6845	-0.0631
	75	0.8872	5.721	4.844	2.222	0.5721	-0.4113	-0.1533	-0.1685

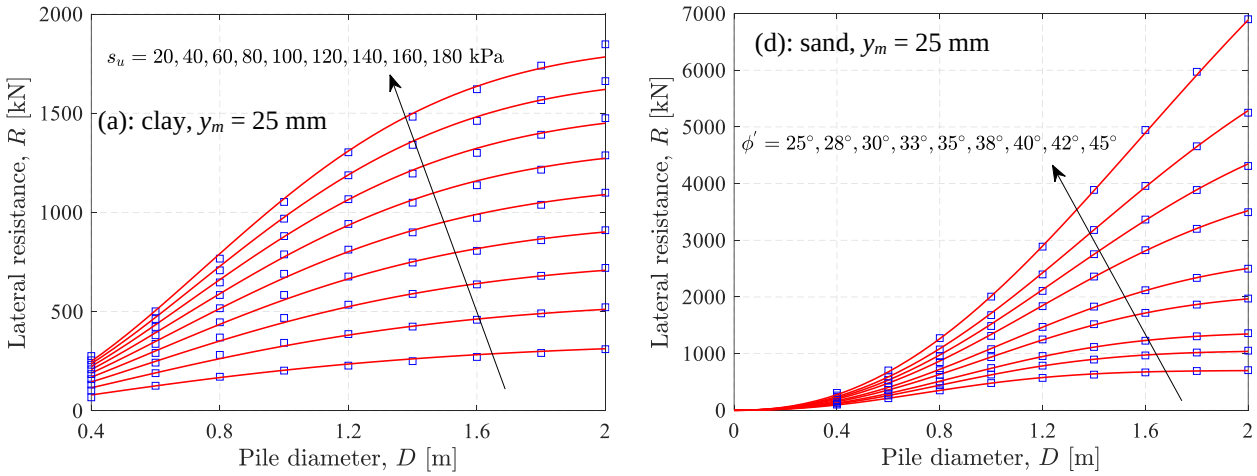

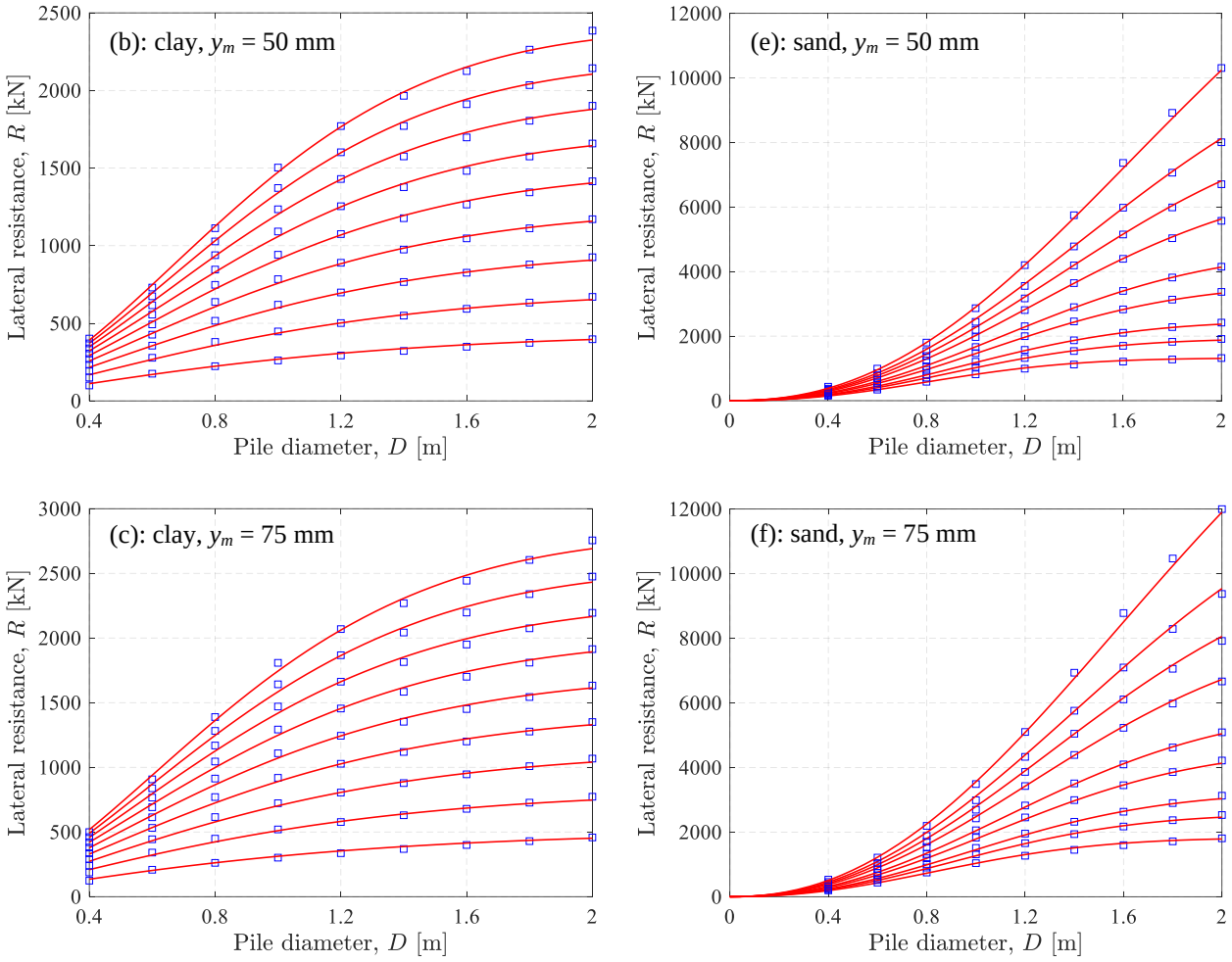

Figure 5. Curve-fitting of finite element results for pile design

Substituting Eq. (10) into the LRFD Eq. (1) at the equality yields

$$\alpha_W \hat{F}_W = \phi_g \hat{a}\left[1-\exp\left(\hat{b}\hat{D}^{\hat{c}}\right)\right] \tag{12}$$

where $\hat{D}$ is the designed pile diameter; $\hat{a}$, $\hat{b}$ and $\hat{c}$ are evaluated using Eq. (11) with the characteristic undrained shear strength, $\hat{s}_u$, and characteristic internal friction angle, $\hat{\phi}'$, in place of s_u and ϕ', respectively. To obtain $\hat{s}_u$ and $\hat{\phi}'$, the soil is sampled over a single column of depth *d* at a distance *s* from the pile location, as shown in Figure 4. It is assumed that *n* observations of the soil shear strength parameters are obtained from the soil sample, i.e., $\hat{s}_u^1, \hat{s}_u^2, \cdots, \hat{s}_u^n$ for clay and $\hat{\phi}_1', \hat{\phi}_2', \cdots, \hat{\phi}_n'$ for sand. As suggested by Fenton and Griffiths (2008), the characteristic undrained shear strength, $\hat{s}_u$, is estimated to be the geometric average of the undrained shear strength observations, i.e. (recall that the s_u random field is lognormally distributed),

$$\hat{s}_u = \left(\prod_{i=1}^{n} \hat{s}_u^i\right)^{1/n} = \exp\left(\frac{1}{n}\sum_{i=1}^{n} \ln \hat{s}_u^i\right) \tag{13}$$

and the characteristic internal friction angle, $\hat{\phi}'$, is taken to be the arithmetic average of the sample observations, i.e.,

$$\hat{\phi}' = \frac{1}{n}\sum_{i=1}^{n}\hat{\phi}_i' \tag{14}$$

The designed pile diameter, $\hat{D}$, is then obtained by re-arranging Eq. (12) to be

$$\hat{D} = \left[\frac{1}{\hat{b}}\ln\left(1-\frac{\alpha_W \hat{F}_W}{\hat{a}\phi_g}\right)\right]^{\frac{1}{\hat{c}}} \tag{15}$$

4 Estimate of failure probability

For a given resistance factor, ϕ_g, and a limiting pile head deflection, y_m, the detailed steps for the estimate of the failure probability are as follows:

(1) Simulate the random fields of the soil strength property, s_u for clay (or ϕ' for sand), having the specified mean, standard deviation and correlation length;

(2) Virtually sample the soil at a distance s from the pile location, and calculate $\hat{s}_u$ (or $\hat{\phi}'$) using Eq. (13) (or Eq. (14));

(3) Design the pile to calculate the designed pile diameter, $\hat{D}$, for the given ϕ_g using Eq. (15);

(4) Obtain the *p-y* curve for each pile node using Figure 2 for clay (or Eq. (6) for sand) with the simulated soil strength values at the pile location;

(5) Evaluate the actual lateral soil resistance, $\bar{R}$, using the finite element *p-y* model, and simulate the lateral wind load having the specified mean and standard deviation;

(6) Check whether the designed pile fails (i.e., $F_W > \bar{R}$) or not against pile deflection; if so, update the number of failures counter, $n_{\text{fail}} = n_{\text{fail}} + 1$;

(7) Repeating steps (1) to (6) n_{sim} times, the probability of failure for the given ϕ_g and y_m is estimated to be $p_f \approx n_{\text{fail}}/n_{\text{sim}}$.

The above overall steps can be repeated for different ϕ_g and y_m, and the failure probability is then estimated as a function of ϕ_g for various values of y_m. The reliability index, β, corresponding to p_f is computed as

$$\beta = \Phi^{-1}\left(1-p_f\right) \tag{16}$$

where Φ is the cumulative distribution function of the standard normal.

5 Results and discussions

5.1 Example

In this example, the mean of the undrained shear strength of clays is taken to be μ_{s_u} =100 kPa, and its coefficient of variation is assumed to be v_{s_u} =0.2, 0.3, and 0.5 (i.e., standard deviations are σ_{s_u} =20, 30 and 50 kPa), which is consistent with the range of v_{s_u} =0.2 to 0.5 suggested by Lee, White, and Ingles (1983). As discussed in Section 2.1, the mean of the internal friction angle of sands is $\mu_{\phi'}$ =35º, and three values of the coefficient of variation are considered, i.e., $v_{\phi'} = 0.05$, 0.10, and 0.15. To investigate the effect of soil correlation length, a range of θ values from 0.1 m to 50 m are chosen.

The wind load is assumed to have a mean of μ_{F_W} =240 kN and a coefficient of variation of v_{F_W} =0.3 (Simiu et al., 2017). As mentioned above, the bias factor of wind loads is taken as k_W=0.78, and thus the characteristic wind load is calculated to be $\hat{F}_W = \mu_W / k_W = 307.7$ kN. According to the NBCC (National Research Council, 2015), the load factor for wind loads, α_W , is equal to 1.4 for ULS, and a value of $\alpha_W = 1.0$ is assumed for SLS.

The two-dimensional soil element is a 0.01×0.01 m square. The pile length and elastic modulus are held constant at 10 m and 35 GPa, respectively. The pile consists of 1000 one-dimensional beam elements, and each element is 0.01 m in length. A total number of n_{sim} =100,000 realizations have been used for each case in the Monte Carlo simulation. Each set of 100,000 realizations took approximately 16 minutes on a desktop computer running on one thread of an AMD 3970X CPU with base clock speed of 3.7 GHz. The soil sampling depth is taken to be the same as the pile length, i.e., d=10 m. Three values of the sampling distance, s, from the pile location are taken, i.e., s=0, 5 m, and 10 m.

All the parameters considered in the analysis are summarized in Table 2.

Table 2. Input parameters used in the Monte Carlo simulation

Undrained shear strength, μ_{s_u} ; σ_{s_u} [kPa]	100; 20, 30, 50
Internal friction angle, $\mu_{\phi'}$; $\sigma_{\phi'}$ [º]	35; 1.75, 3.50, 5.25
Soil unit weight, γ [kN/m^3]	20

Allowable deflection, y_m [mm]	25, 50, 75
Wind load, μ_{F_W} ; ν_{F_W} [kN]	240; 72
Bias factor of wind load, k_W	0.78
Wind load factor, α_W	1.4 (ULS), 1.0 (SLS)
Soil sampling distance and depth, s; d [m]	0, 5, 10; 10
Correlation length, θ [m]	0.1 m to 50 m
p-y parameters for clay, J; ε_{50}	0.5; 0.01
Soil and pile element size, Δx; Δy [m]	0.01; 0.01
Pile length, L [m]	10
Pile elastic modulus, E_p [GPa]	35
Number of simulations, n_{sim}	100,000

5.2 Results and discussions

5.2.1 Effect of limiting pile head deflections

Figure 6 shows the effect of the limiting pile head deflection on the calculated failure probability for medium soil variability (i.e., $\nu_{s_u} = 0.3$ for clay and $\nu_{\phi'} = 0.10$ for sand) and s=5 m and θ=10 m. Since the primary difference between ULS and SLS is the load factor for wind loads, the estimated curves for ULS are expected to be similar to those for SLS except for the failure probability values. Thus, only ULS results are presented here as an example. In addition, as the failure probabilities for ULS cases with ϕ_g=0.4, 0.5, and 0.6 are too small to be accurately assessed using only 100,000 realizations, a total number of realizations of n_{sim}=1,000,000 is used for these ULS cases. Using 1,000,000 independent realizations, the estimated failure probability, $\hat{p}_f$, has a standard error $\sqrt{\hat{p}_f\left(1-\hat{p}_f\right)/n_{\text{sim}}}$, which for a failure probability of 10^{-5} is 3.16×10^{-6}.

Figure 6 shows that the limiting pile deflection has a negligible effect on the failure probability for either clay or sand, as expected, because the limiting pile head deflection just affects the designed pile diameter, and the failure probability is primarily governed by the soil variability. In addition, the failure probability for clay is

close to that for sand. This results in a potential merit for the calibration of resistance factors: consistent resistance factors may be applied for clay and sand, which is discussed in the following section.

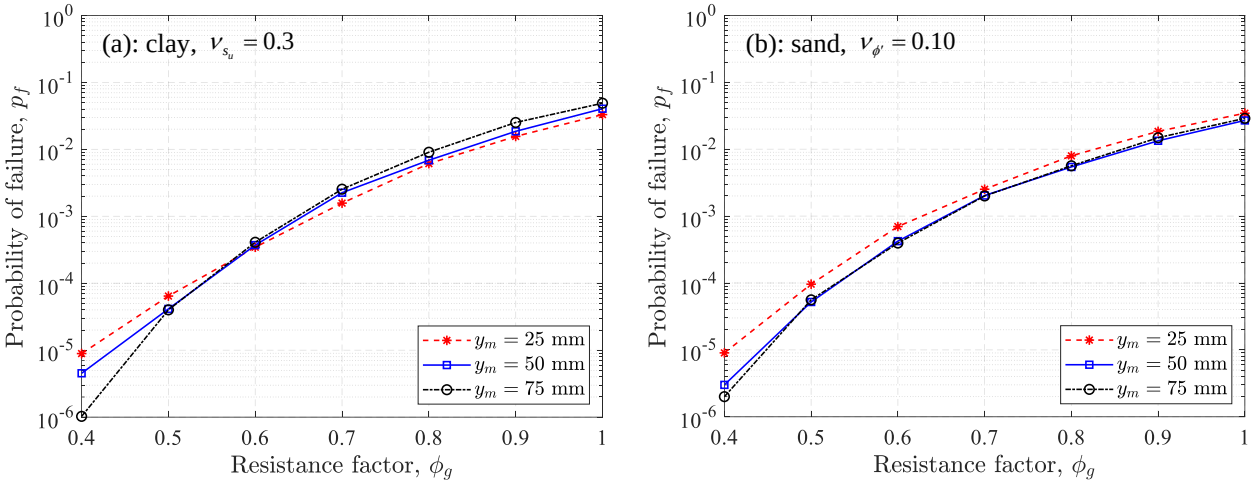

Figure 6. Estimated ULS p_f as a function of ϕ_g for different limiting pile deflections (θ=10 m, s=5 m)

5.2.2 Effect of correlation lengths

Figure 7 illustrates the effect of the soil correlation length on the estimated failure probability for different soil variabilities and sampling distances using the limiting pile head deflection of y_m=75 mm. The resistance factor of ϕ_g=0.7 is taken as an example. The figure shows the existence of a "worst case" correlation length for all the cases, which has also been found in the ULS design (e.g., Fenton et al., 2008) and SLS design (e.g., Nour et al., 2002; Fenton and Griffiths, 2002; Fenton et al., 2005) of shallow foundations, the SLS design of deep foundations (e.g., Naghibi et al., 2014), and the design of retaining walls (e.g., Fenton et al., 2005). Assuming stationary random soil properties (i.e., having the same mean and standard deviation everywhere in the soil mass), a very small correlation length results in reduced variance in the sample average (i.e., $\hat{s}_u$ for clay and $\hat{\phi}'$ for sand), that is, less difference between the characteristic soil properties and the average of the soil properties at the location of the designed pile. Similarly, a very large correlation length implies that the soil properties at the sampling location and at the designed pile location are very similar. Both conditions lead to a relatively high understanding of the soil condition at the pile location and thus low failure probabilities. Between these two extremes, the failure probability increases to a maximum at the "worst case" correlation length. An implication of this is that the "worst case" correlation length can be used for conservative design, particularly when an accurate estimate of the correlation length is not available.

It can be seen that the soil variability has a significant impact on the estimated failure probability, as expected. In addition, a smaller sampling distance considerably diminishes the failure probability, also as expected due

to higher understanding of the soil properties at the pile location. More specifically, for $\nu_{s_u} = 0.3$, the failure probability at θ=10 m for the case of s=5 m is about three times that for s=0. It should also be noted that the failure probability for s=10 m is just about 1.4 times that for s=5 m, suggesting that a sampling distance smaller than the intermediate value has a greater potential to reduce the failure probability, that is, the failure probability is more sensitive to smaller sampling distances.

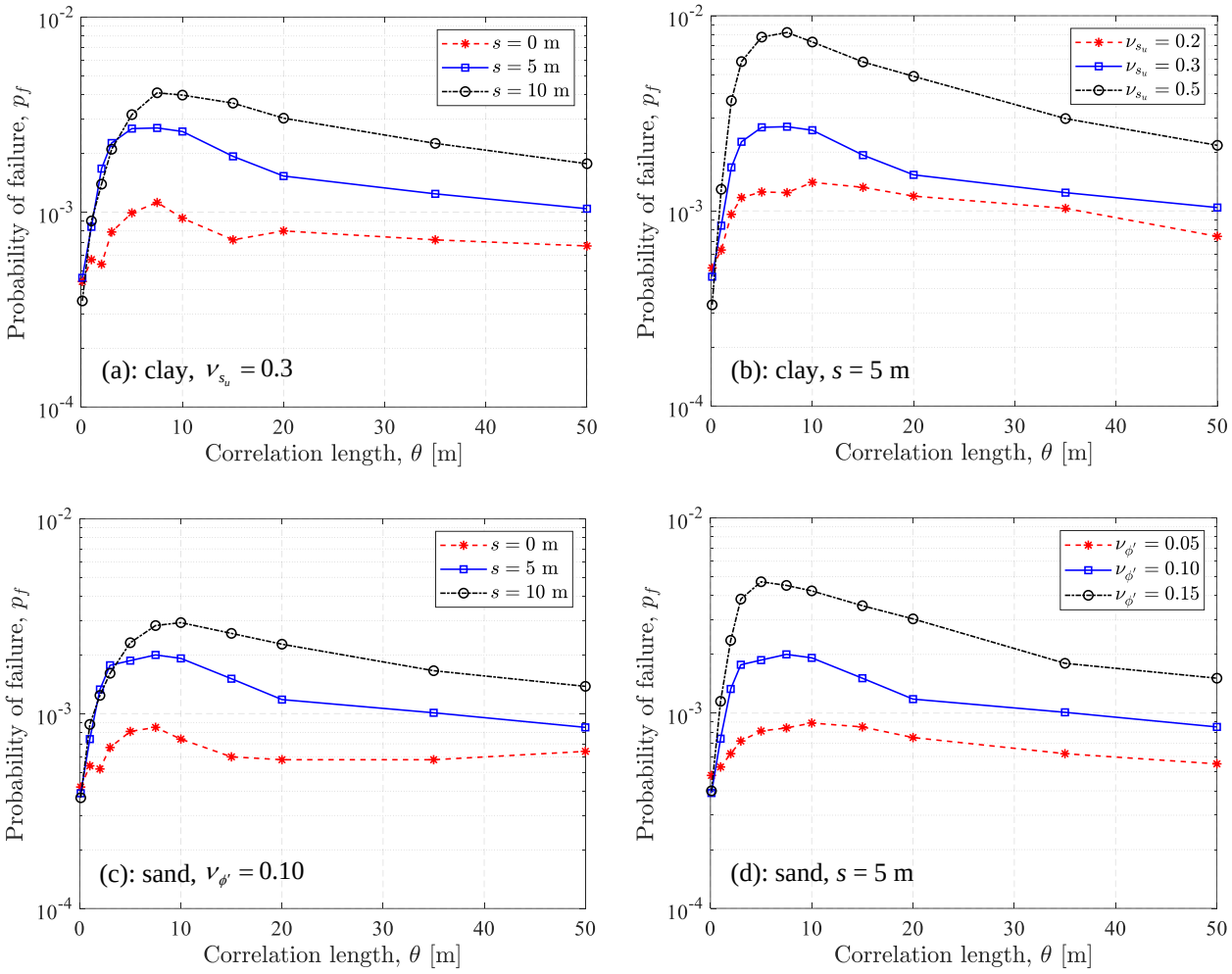

Figure 7. Estimated ULS p_f as a function of θ for different sampling distances and soil coefficients of variation (ϕ_g=0.7, y_m=75 mm)

As shown in Figure 7, although the soil coefficient of variation and the sampling distance have great effects on the failure probability, they have a minor effect on the "worst case" correlation length. The "worst case" correlation length for the above cases is always about 5 m to 10 m, which is approximately equal to or somewhat less than the pile length L=10 m. To investigate the effect of pile length on the "worst case" correlation length, the ULS failure probabilities for pile lengths of L=5 m and 20 m are also estimated for comparison, as shown in Figure 8. Note that the fitted equations for design in Section 3 are not applicable for L=5 m and 20 m, and therefore, a similar procedure of curve-fitting was separately performed for L=5 m and

20 m. The calculated results and the corresponding fitting equations are not shown here for brevity. For simplicity, only the results for clay with $\nu_{s_u} = 0.3$ are presented.

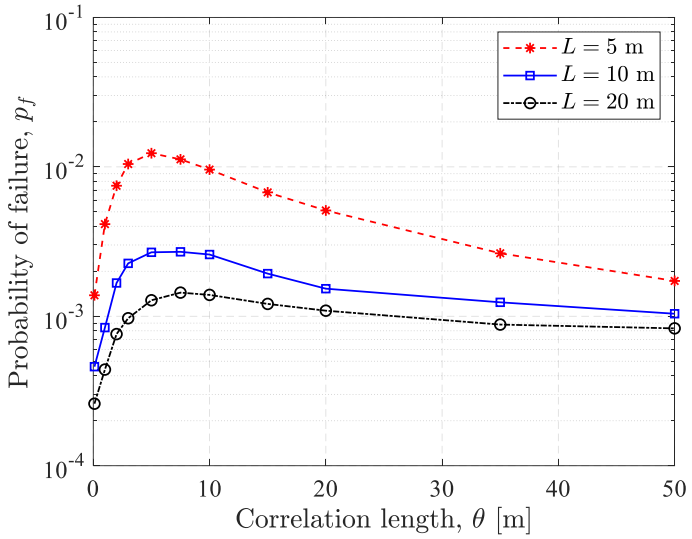

Figure 8. Estimated clay ULS p_f for different pile lengths ($\nu_{s_u} = 0.3$, ϕ_g=0.7, y_m=75 mm)

It can be seen from Figure 8 that the "worst case" correlation length for L=5 m is the same as its pile length, while the pile of L=20 m has a similar "worst case" correlation length (5 m to 10 m) to the pile of L=10 m. This may be primarily attributed to the fact that the significant lateral deflections of a laterally loaded pile typically occur within a depth equal to eight to ten pile diameters (Duncan et al., 1994).

For L=10 m, substituting the factored design wind load, $\alpha_W \hat{F}_W$ =430.8 kN, the mean undrained shear strength, μ_{s_u} =100 kPa, and the resistance factor, ϕ_g=0.7, into Eq. (15) gives a designed pile diameter $\hat{D}$ =0.6 m, resulting in 10 $\hat{D}$ =6 m, close to the "worst case" correlation length for L=10 m and 20 m. Therefore, the "worst case" correlation length is expected to be close to the pile length involved in the pile deflection resistance. In other words, when the pile length is less than 10 pile diameters, the entire pile length is involved in pile deflection behavior, and the "worst case" correlation length is close to the actual pile length; when the pile length is greater than 10 pile diameters, the "worst case" correlation length is likely to be the close to 10 pile diameters and a longer pile length makes only a small difference.

5.2.3 Effect of sampling distances

Figure 9 presents the estimated ULS failure probability as a function of resistance factor for θ=10 m and different soil sampling distances. As seen in Figure 9, although a total number of realizations of n_{sim}=1,000,000

is used for the ULS cases with ϕ_g=0.4, 0.5, and 0.6, the failure probabilities for some cases with ϕ_g=0.4 are still too small to be accurately estimated.

Figure 9(a) and (d) shows that the soil variability has a great effect on the failure probability. More specifically, for clay with an intermediate sampling distance of s=5 m, the failure probabilities for ν_{s_u} =0.2, 0.3, and 0.5 are 1.20×10^{-5}, 4.13×10^{-5}, and 4.83×10^{-4}, respectively. However, it should also be noted that the effect of the soil variability is gradually reduced with a decrease in the soil sampling distance. In particular, when the soil sampling location is at the pile location (i.e., s=0), the effect of soil coefficient of variability becomes very small. The primary reason for this is that when the soil sampling distance decreases (i.e., the soil sample column is closer to the pile location), the design soil parameters estimated from the soil samples are more likely to be closer to those "seen" at the pile location, thereby reducing the effect of soil variability.

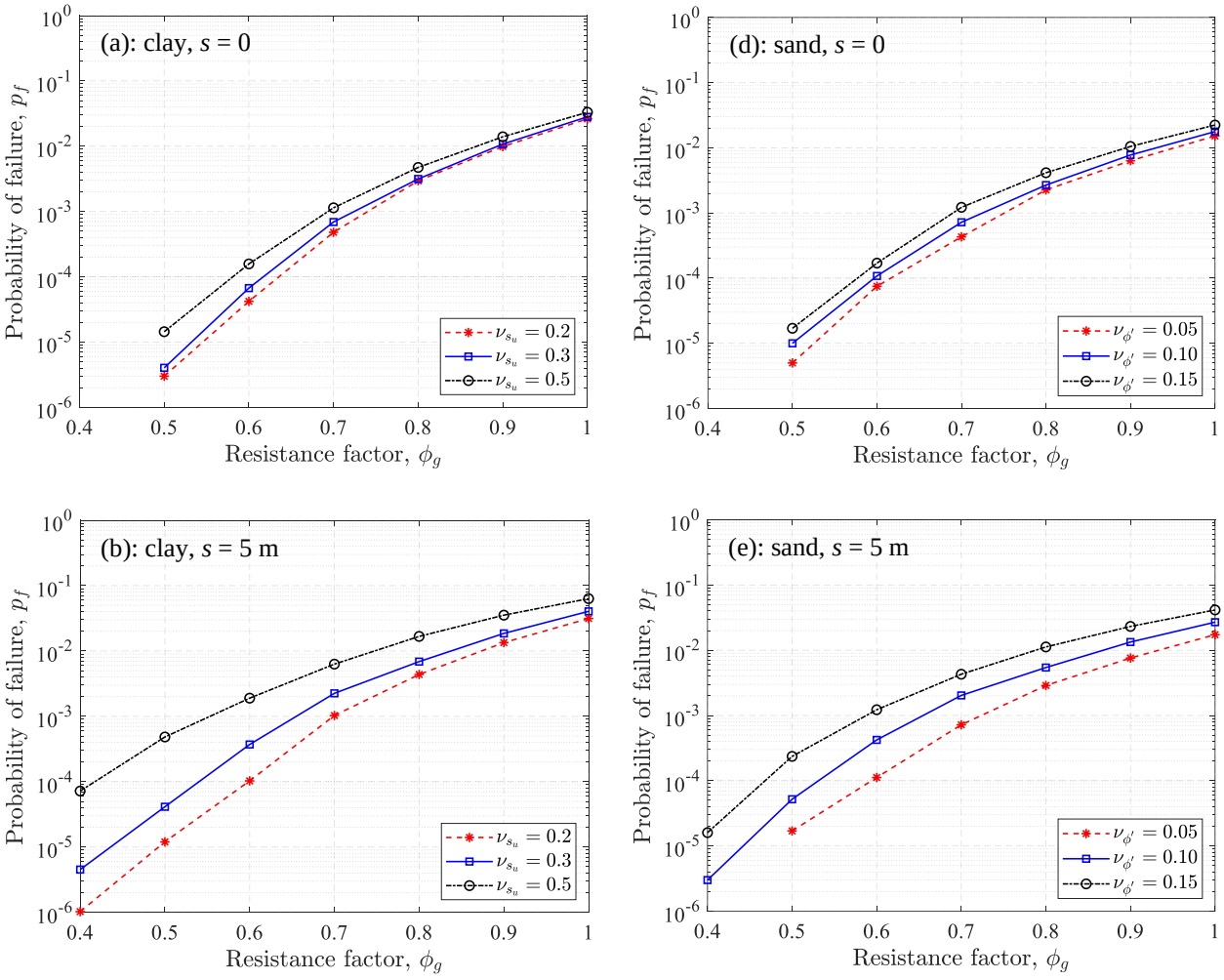

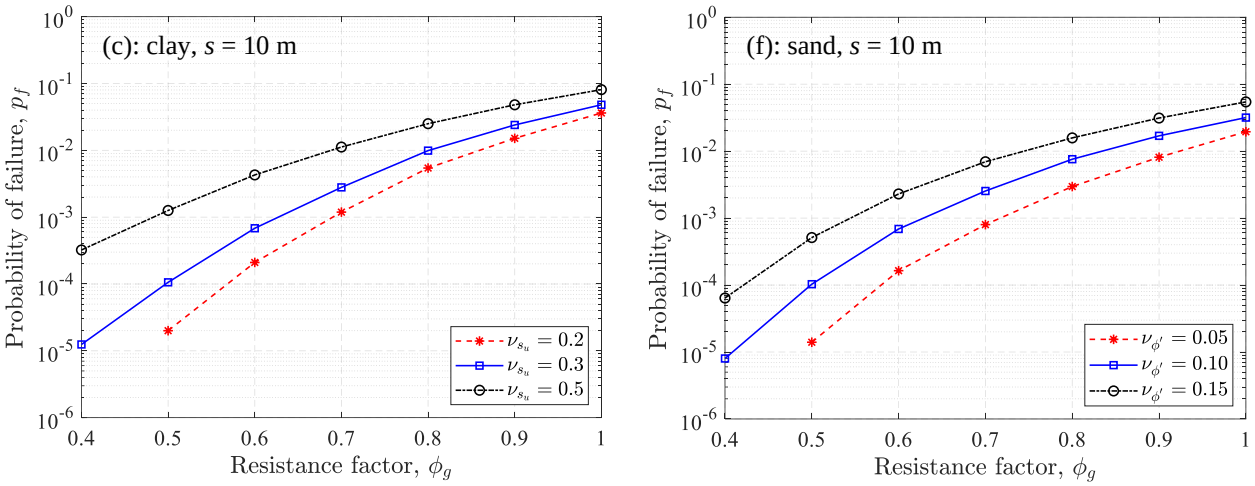

Figure 9. Estimated ULS p_f as a function of ϕ_g for different sampling distances (θ=10 m, y_m=50 mm)

5.2.4 Required resistance factors for design

To determine the required resistance factors for the design against pile deflections (ULS and SLS), the estimated failure probabilities for different soil sampling distances are compared to the target lifetime failure probabilities. As shown in Figure 10, only typical cases for the medium soil variability (i.e., $\nu_{s_u} = 0.3$ for clay and $\nu_{\phi'} = 0.10$ for sand) and medium limiting pile head deflection (i.e., y_m=50 mm) are presented. In addition, only the correlation length of 10 m is considered as it is close to the "worst case" value. For ULS, the range of the target lifetime reliability index (i.e., β_m=2.8 → $p_m = 2.6\times10^{-3}$ to β_m=3.5 → $p_m = 2.3\times10^{-4}$) recommended by Becker (1997a; 1997b) for the NBCC (National Research Council, 2015) is applied, as seen in Figure 10(a) and (c). For SLS, the maximum acceptable lifetime failure probabilities, 10^{-1} to 10^{-3}, are also superimposed in Figure 10(b) and (d).

As can be seen from Figure 10(a) and (c), the required resistance factor for ULS ranges from 0.55 to 0.78. To be more specific, taking $p_m = 2.3\times10^{-4}$ and s=5 m, the required resistance factor is about 0.58 for both clay and sand, which is slightly larger than the value of ϕ_g = 0.50 recommended by the CHBDC (CSA, 2019). This means that pile ULS design against deflections based on the CHBDC (CSA, 2019) is conservative.

According to Figure 10(b) and (d), the required SLS resistance factor is around 0.45 to 0.85 for clay and 0.45 to 0.94 for sand. If $p_m = 0.01$ and s=5 m are taken, the required SLS resistance factor is about 0.60 for both clay and sand, which is smaller than the recommendation of ϕ_g=0.80 by the CHBDC (CSA, 2019), indicating unconservative pile SLS design against deflections. Considering that practical structures are usually supported

by multiple individual foundations and that the practical correlation length is unlikely to be close to the "worst case" correlation length considered here, the recommendation of ϕ_g=0.80 might be reasonable.

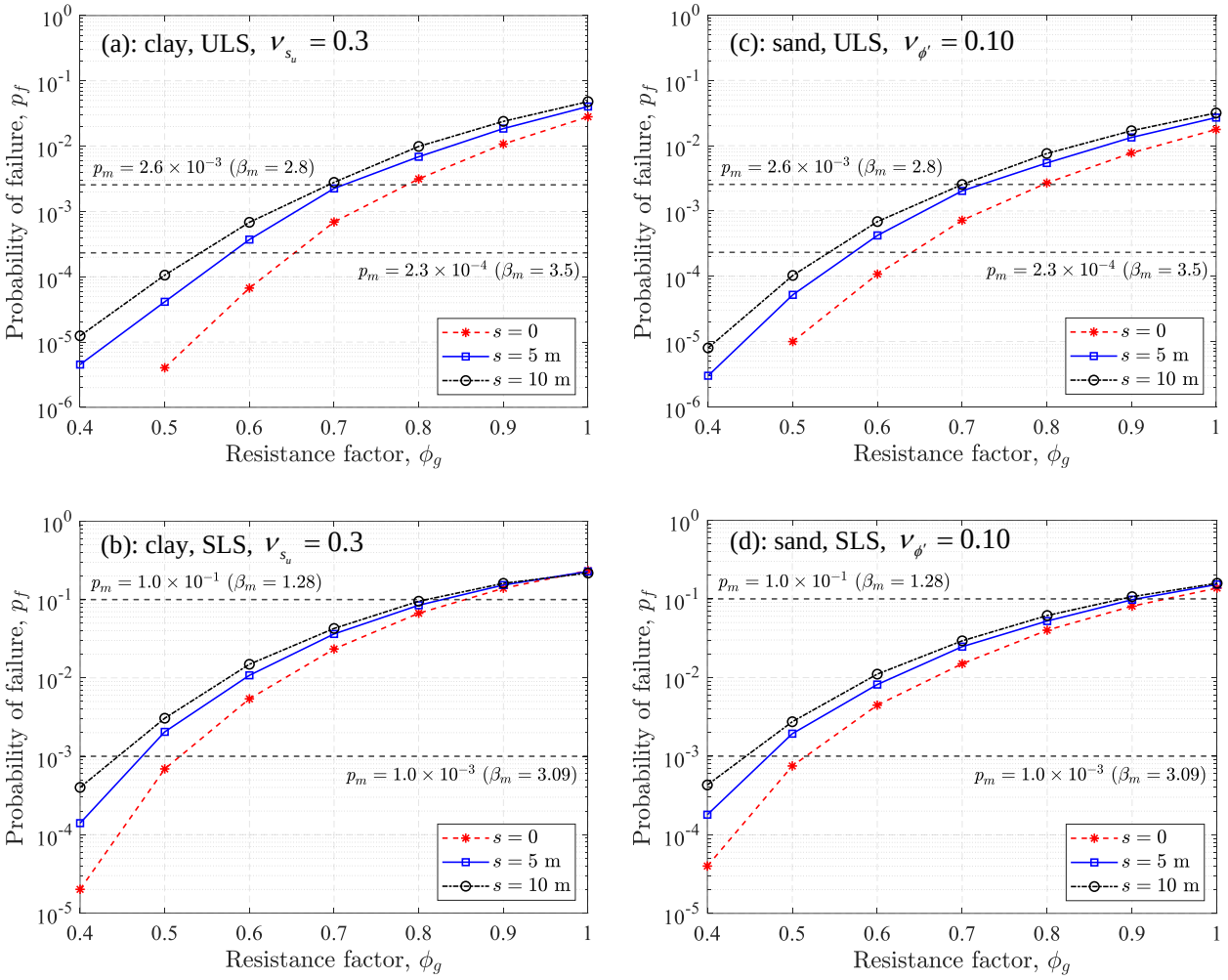

Figure 10. Required resistance factors for target failure probabilities (θ=10 m, y_m=50 mm)

6 Conclusions

This paper carried out a reliability analysis of pile design against lateral deflections under wind loading through the Random Finite Element Method. The ULS and SLS design for both cohesive and frictional soils were considered. The widely-used *p-y* method was employed to compute the lateral soil reaction by considering spatially random soil properties. In the analysis, the designed pile diameter was first determined using the LRFD approach, and then Monte Carlo simulations were used to estimate the failure probability of the design. Parametric studies were also performed to investigate the effects of the limiting pile head deflection, correlation length, soil sampling distance, and soil variability on the estimated failure probability. In addition, the required resistance factors for ULS and SLS have been estimated by comparing the estimated failure probability to the target failure probability levels.

As expected, the effect of the limiting pile head deflection on the required resistance factor is negligible. The results indicate the existence of a "worst case" correlation length, which is dependent on the pile length. The soil variability considerably affects the estimated failure probability, but its effect is gradually reduced as the soil sampling distance decreases. Considering the cases with an intermediate soil coefficient of variation and a medium understanding of the soil condition (i.e., s=5 m), the required resistance factor for ULS design was found to range from 0.55 to 0.78, and the choice of ϕ_g=0.50 by the CHBDC (CSA, 2019) appears to be relatively conservative. If the target lifetime failure probability of 0.01 is desired for SLS, the required resistance factor was found to be approximately 0.60 for both clay and sand, indicating that the recommendation of ϕ_g=0.80 by the CHBDC (CSA, 2019) is unconservative. However, for practical structures supported by a pile system, the value of ϕ_g=0.80 might still be an acceptable choice. The reliability analysis of a redundant pile system requires further research.

In this study, only one soil sample column was considered, whereas multiple sample columns are expected in practice, which may help reduce the estimated failure probability. In addition, compared to a single pile, a group pile system will likely result in much lower system failure probability. On the other hand, the pile properties (i.e., elastic modulus and diameter) were assumed to be deterministic, thereby underestimating the failure probability. However, since the uncertainty associated with the soil is greater than that related to the pile, the pile uncertainties are believed to have a limited effect on the calculated failure probability. As mentioned previously, the soil properties at the pile location are taken as the average soil properties in the soil cells on either side of the pile to generate the *p-y* curves. Since the horizontal size of the soil influence zone is much smaller than the "worst case" and practical correlation lengths, this simplification is believed to be reasonable for medium soil correlation lengths and above. In general, these conservative and unconservative factors cancel one another out to some extent. Moreover, a wide range of the target lifetime failure probability is considered in the analysis, and thus research into more accurate reliability targets can facilitate the calibrated resistance factors. Overall, the current results can be used to guide the calibration of pile design against lateral deflections.

7 Acknowledgements

The authors would like to acknowledge the financial support provided by the Canadian Standard Association Group Research Project Award and Mitacs (Grant No.: IT21047), and the Natural Sciences and Engineering Research Council of Canada.

References

American Association of State Highway and Transportation Officials, 2020. AASHTO LRFD Bridge Design Specifications, 9th ed. Washington.

API, 2014. API Recommended Practice 2GEO, Geotechnical and Foundation Design Considerations, 1st ed. American Petroleum Institute (API), Washington.

Barker, R.M., Duncan, J.M., Rojiani, K.B., Ooi, P.S.K., Tan, C.K., Kim, S.G., 1991. Appendix A: Procedures for evaluating performance factors. Load factor design criteria for highway structure foundations. Final Report, NCHRP 24-4. National Cooperative Highway Research Program.

Becker, D.E., 1997a. Eighteenth Canadian geotechnical colloquium: Limit states design for foundations. Part I. An overview of the foundation design process. Can. Geotech. J. 33(6), 956-983. doi: 10.1139/t96-124.

Becker, D.E., 1997b. Eighteenth Canadian geotechnical colloquium: Limit states design for foundations. Part II. Development for the national building code of Canada. Can. Geotech. J. 33(6), 984-1007. doi: 10.1139/t96-125.

Burgess, J., Fenton, G.A., Griffiths, D.V., 2019. Probabilistic seismic slope stability analysis and design. Can. Geotech. J. 56(12): 1979-1998. doi: 10.1139/cgj-2017-0544.

Cami, B., Javankhoshdel, S., Phoon, K.K., Ching, J., 2020. Scale of fluctuation for spatially varying soils: estimation methods and values. ASCE ASME J. Risk Uncertain. Eng. Syst. A Civ. Eng. 6(4), 03120002.

CFEM, 2006. Canadian foundation engineering manual, 4th ed. Canadian Geotechnical Society, Richmond, Canada.

CSA, 2019. S6-19 Canadian Highway Bridge Design Code. Canadian Standards Association (CSA), Toronto, Canada.

Duncan, J.M., Evans Jr, L.T. Ooi, P.S., 1994. Lateral load analysis of single piles and drilled shafts. J. Geotech. Eng. 120(6), 1018-1033.

Ellingwood, B., 1981. Wind and snow load statistics for probabilistic design. J. Struct. Div. 107(7), 1345-1354.

Ellingwood, B., MacGregor, J.G., Galambos, T.V., Cornell, C.A., 1982. Probability based load criteria: load factors and load combinations. J. Struct. Div. 108(5), 978-997.

Fenton, G.A., Griffiths, D.V., 1993. Statistics of block conductivity through a simple bounded stochastic medium. Water Resour. Res. 29(6), 1825-1830. doi: 10.1029/93WR00412.

Fenton, G.A., Griffiths, D.V., 2002. Probabilistic foundation settlement on spatially random soil. J. Geotech. Geoenviron. Eng. 128(5), 381-390.

Fenton, G.A., Griffiths, D.V., 2007. Reliability-based deep foundation design. Probabilistic Applications in Geotech. Eng. 1-12.

Fenton, G.A., Griffiths, D.V., 2008. Risk assessment in geotechnical engineering. John Wiley & Sons, New York.

Fenton, G.A., Griffiths, D.V., Cavers, W., 2005. Resistance factors for settlement design. Can. Geotech. J. 42(5), 1422-1436. doi: 10.1139/t05-053.

Fenton, G.A., Griffiths, D.V., Williams, M.B., 2005. Reliability of traditional retaining wall design. Géotechnique 55(1), 55-62.

Fenton, G.A., Griffiths, D.V., Zhang, X., 2008. Load and resistance factor design of shallow foundations against bearing failure. Can. Geotech. J. 45(11), 1556-1571. doi: 10.1139/T08-061.

Fenton, G.A., Vanmarcke, E.H., 1990. Simulation of random fields via local average subdivision. J. Eng. Mech. 116(8), 1733-1749. doi: 10.1061/(ASCE)0733-9399(1990)116:8(1733).

Foye, K.C., Abou-Jaoude, G., Prezzi, M., Salgado, R., 2009. Resistance factors for use in load and resistance factor design of driven pipe piles in sands. J. Geotech. Geoenviron. Eng. 135(1), 1-13.

Griffiths, D.V., Fenton, G.A., 1993. Seepage beneath water retaining structures founded on spatially random soil. Géotechnique 43(4), 577-587. doi: 10.1680/geot.1993.43.4.577.

Griffiths, D.V., Paiboon, J., Huang, J., Fenton, G.A., 2013. Reliability analysis of beams on random elastic foundations. Géotechnique 63(2), 180-188.

Haldar, S., Sivakumar Babu, G.L., 2008. Load resistance factor design of axially loaded pile based on load test results. J. Geotech. Geoenviron. Eng. 134(8), 1106-1117.

Kim, G., Kim, D., Lee, J., 2021. Resistance factors for LRFD of laterally loaded drilled shafts in sands characterized for transmission line structures. J. Geotech. Geoenviron. Eng. 147(5), 04021017.

Kim, G., Lee, J., 2022. Load and Resistance Factor Design for Serviceability Limit State of Laterally Loaded Drilled Shafts for Transmission Line Structures in Sands. J. Geotech. Geoenviron. Eng. 148(1), 04021166.

Kwak, K., Kim, K.J., Huh, J., Lee, J.H., Park, J H., 2010. Reliability-based calibration of resistance factors for static bearing capacity of driven steel pipe piles. Can. Geotech. J. 47(5), 528-538.

Lee, I.K., White, W., Ingles, O.G., 1983. Geotechnical Engineering. Pitman, London.

Low, B.K., 2020. Geotechnical insights from reliability-based design to improve partial factor design methods. In Geo-Congress 2020: Engineering, Monitoring, and Management of Geotechnical Infrastructure (pp. 686-695). Reston, VA: American Society of Civil Engineers.

Matlock, H., 1970. Correlations for design of laterally loaded piles in soft clay. Proceedings of the II Annual Offshore Technology Conference, Houston, Texas, (OTC 1204): 577-594.

McClelland, B., Focht Jr, J.A., 1958. Soil modulus for laterally loaded piles. Trans. Am. Soc. Civil Eng. 123(1), 1049-1063.

Naghibi, F., Fenton, G.A., Griffiths, D.V., 2014. Serviceability limit state design of deep foundations. Géotechnique 64(10), 787-799.

Naghibi, M., Fenton, G.A., 2011. Geotechnical resistance factors for ultimate limit state design of deep foundations in cohesive soils. Can. Geotech. J. 48(11), 1729-1741.

National Research Council of Canada. 2015. National Building Code of Canada, 14th ed. National Research Council of Canada, Ottawa.

Nour, A., Slimani, A., Laouami, N., 2002. Foundation settlement statistics via finite element analysis. Comput. Geotech. 29(8), 641-672. doi: 10.1016/S0266-352X(02)00014-9.

Phoon, K.K., Kulhawy, F.H., 1999. Characterization of geotechnical variability. Can. Geotech. J. 36(4), 612-624. doi: 10.1139/t99-038.

Phoon, K.K., Kulhawy, F.H., Grigoriu, M.D., 2000. Reliability-based design for transmission line structure foundations. Comput. Geotech. 26(3-4), 169-185. doi: 10.1016/S0266-352X(99)00037-3.

Puła, W., Griffiths, D.V., 2021. Transformations of spatial correlation lengths in random fields. Comput. Geotech. 136, 104151. doi: 10.1016/j.compgeo.2021.104151.

Simiu, E., Pintar, A.L., Duthinh, D., Yeo, D., 2017. Wind load factors for use in the wind tunnel procedure. ASCE-ASME Journal of Risk and Uncertainty in Engineering Systems, Part A: Civil Engineering, **3**(4), 04017007. doi: 10.1061/AJRUA6.0000910.

Smith, I.M., Griffiths, D.V., 1988. Programming the finite element method, second ed. John Wiley & Sons, New York.

Tang, C., Phoon, K.K., 2018. Statistics of model factors and consideration in reliability-based design of axially loaded helical piles. J. Geotech. Geoenviron. Eng. 144(8), 04018050.

Vanmarcke, E., 2010. Random fields: analysis and synthesis. World scientific, Singapore.